PHYSICAL REVIEW D VOLUME 19, NUMBER 3 1 FEBRUARY 1979

Electromagnetic production of trimuons in deep-inelastic muon scattering

V. Ganapathi and J. Smith
Institute for Theoretical Physics, State University of New York at Stony Brook, Stony Brook, New York 11794
(Received 6 September 1978)

We calculate the cross sections for the electromagnetic contribution to the reaction $\mu + N \to 3\mu + N$, using the radiative quark-parton model. We discuss some features of the reactions which are expected experimentally, and helpful in distinguishing Compton production from muon radiative production.

I. INTRODUCTION

Trilepton production by lepton beams has been under consideration for a long time. The earliest calculations were performed for electrons, to test the validity of quantum electrodynamics. These calculations were carried out for scattering off a fixed target nucleus and for specific kinematic configurations.[1] Later a more detailed investigation for muon production of electron-positron pairs was carried out by Brodsky and Ting.[2] This was followed by a calculation of muon tridents by Tannenbaum,[3] to see the effects of Fermi-Dirac statistics for muons. The experiment of Russell *et al.*[4] verified for the first time that muons obey Fermi-Dirac statistics.

The advent of the quark-parton model[5] provided a theoretical framework for the analysis of deep-inelastic scattering. Bjorken and Paschos[6] then proposed that the quark-parton model could be tested further in the inelastic photoproduction of muon pairs. In this reaction they assumed that only diagrams where the same quark absorbs and emits radiation are important. Experiments to verify this were conducted by Davis *et al.*[7] After taking into account the Bethe-Heitler production of muon pairs, they found that the cross sections were still much larger than predicted. A similar conclusion was reached for an experiment of inelastic Compton scattering by Caldwell *et al.*[8]

Since the building of the accelerators at Fermilab and CERN, high-energy neutrino and muon beams have been used to yield a large amount of data. The charged-current interaction of neutrinos has verified qualitatively the scaling predictions of the quark-parton model.[9] Dimuon production by neutrinos has yielded further information on hadronic processes.[10] Finally trimuon events in neutrino and antineutrino experiments have been observed by the Caltech-Fermilab,[11] Fermilab-Harvard-Pennsylvania-Rutgers-Wisconsin,[12] and CERN-Dortmund-Heidelberg-Saclay[13] (CDHS) groups at Fermilab and CERN. Detailed phenomenological analyses has been carried out for these processes.[14] One of the mechanisms investigated is the radiative production of trimuons.[15,16] In this calculation it was assumed that radiative muon pair production occurs off the muon and quark lines. There are three diagrams which must be taken together to preserve gauge invariance. Though there are other processes which contribute to trimuon production, the improved statistics of the CDHS group[17] show that the radiative process accounts for approximately one third of their events. Thus the existence of radiative processes has been verified.

Experiments of Chang *et al.*[18] at Fermilab, have observed trimuons in deep-inelastic muon scattering. They reported a rate larger than the normal QED processes. It was proposed that this may be due to associated production of charm[19] and seems to explain the data.

However, in view of the observation of radiative effects in neutrino production of trimuons, it seems worthwhile to investigate the corresponding process for muon production of trimuons. In investigating the electromagnetic production of trimuons, there are three distinct processes we can consider. The first is the Bethe-Heitler production [Fig. 1(a)]. The second is radiative production by muons [Fig. 1(b)]. The last is radiative production by quarks [Fig. 1(c)]. We have considered only the last two in this paper. These are the analogs of the corresponding processes considered in the neutrino case. However, unlike the neutrino case we can consider these two sets of diagrams separately, as they are individually gauge invariant. In this fashion the former processes, which are pure QED backgrounds, can be isolated to yield information on processes occuring at the hadronic vertex. This also provides a check of the quark-parton model.

The Bethe-Heitler muon pairs are produced in an even-charge-conjugation state, whereas in muon and quark radiative production, the muon pairs are in an odd-charge-conjugation state. The Bethe-

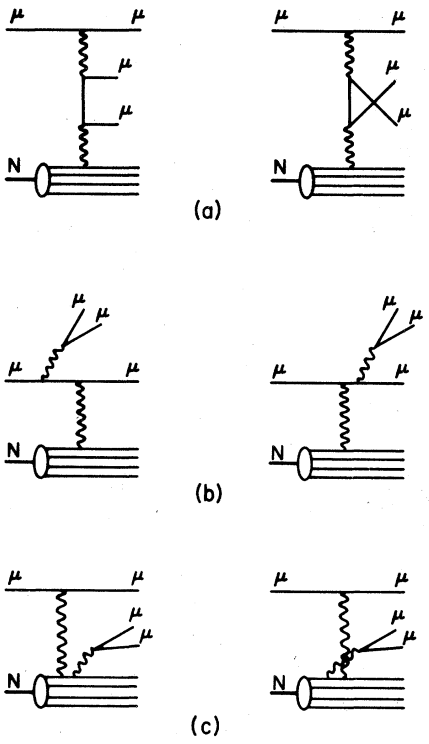

FIG. 1. Diagrams for electromagnetic production of trimuons: (a) Bethe-Heitler process, (b) muon radiative production, (c) Compton production.

Heitler production has been seen in the trident experiments,[4] and they involve very low momentum transfers to the nucleus, and thus by a suitable choice of cuts can be eliminated.

The muon pair production cross section from the diagrams where the quark radiates, which is virtual Compton process, is expected to be much smaller than the cross section where the muon radiates. However, by suitably imposed cuts on certain variables, we can hopefully isolate the Compton process, and see how the predictions compare with the data. Thus one can also subtract the radiative process in the event that there is a larger cross section for hadronic muon-pair production. We now briefly discuss such contributions.

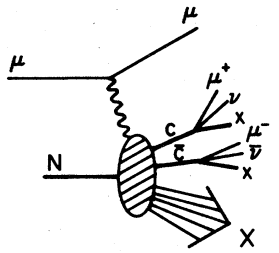

FIG. 2. Associated production of charm, producing trimuons.

As mentioned earlier associated production of charm was used to explain the existing trimuon data. This calculation[19] was done assuming diffractive production (small x) of a pair of charmed particles, which subsequently decayed semileptonically producing muons (Fig. 2). Calculations for the associated production of charm can be done within the framework of the quark-parton model. There are two classes of diagrams which produce $c\bar{c}$. In the first, the photon couples directly to the $c\bar{c}$ [Fig. 3(a)] and in the second, the photon excites the quark which produce the $c\bar{c}$, either by annihilation of gluons arising from different quarks [Fig. 3(b)], or by gluon brehmsstrahlung [Fig. 3(c)].

Further contributions are expected from the production of mesons which decay into two muons. If these are electromagnetically produced [Fig. 4(a)], when the muon momentum transfer becomes small (low q^2), we can correlate this to photoproduction of muon pairs [Fig. 4(b)]. In this way an idea of low-q^2 events can be obtained from photoproduction experiments.

At present, data on the photoproduction of muon pairs is rather meager,[7] and the signal is much larger than expected. The production of mesons

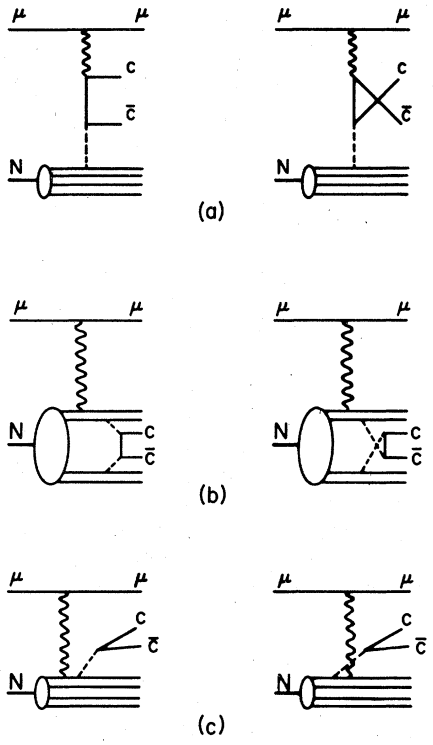

FIG. 3. Diagrams for associated production of charm in the quark-parton model: (a) diffractive production, (b) gluon annihilation, (c) brehmstrahlung.

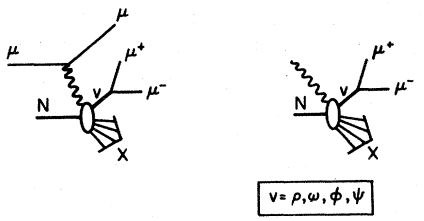

FIG. 4. Electroproduction and photoproduction of muon pairs.

decaying into two muons is unable to account for the signal. Though associated charm photoproduction is expected to be $\frac{1}{2}\%$ of the total photoproduction cross section,[20,21] these probably will not account for the entire cross section. In this connection, we mention the data on *low-mass* muon-pair production in pp and πp collisions,[22] which has a much larger signal than expected on the basis of current models. This poorly understood mechanism is reflected in the neutrino production of trimuons (replacing the pion by a virtual W boson, for the axial-vector current) and accounts for approximately $\frac{2}{3}$ of the trimuon cross section.[17] We expect, therefore, that the vector current behaves similarly and this will yield a large cross section for the production of low-mass dimuons in photoproduction and muoproduction. Hence this mechanism yields a possible explanation of the large signal.[7] This connection is currently under investigation. However, in this paper we concentrate on the pure electromagnetic process.

The plan of the paper is as follows: In Sec. II we present the details of the calculation. In Sec. III we discuss the distributions obtained and in Sec. IV give our conclusions.

II. CALCULATION

The three processes responsible for the electromagnetic production were indicated in the Introduction (Fig. 1). The dominant contributions to the matrix element arise when the virtual momenta are close to their mass shell values. Thus, for the following reason, the Bethe-Heitler process [Fig. 1(a)] contributes to an entirely different region of phase space than the other two [Figs. 1(b) and 1(c)]. The former has two spacelike photon propagators whereas the latter only have one. The other timelike propagator cannot get close to its mass shell as it must produce two muons. Now, the computer programs used are less accurate in evaluating the cross sections, when there are many severe peakings in the variables. We thus neglect the Bethe-Heitler process. We feel we are justified in so doing because of the reasons mentioned in the introduction.

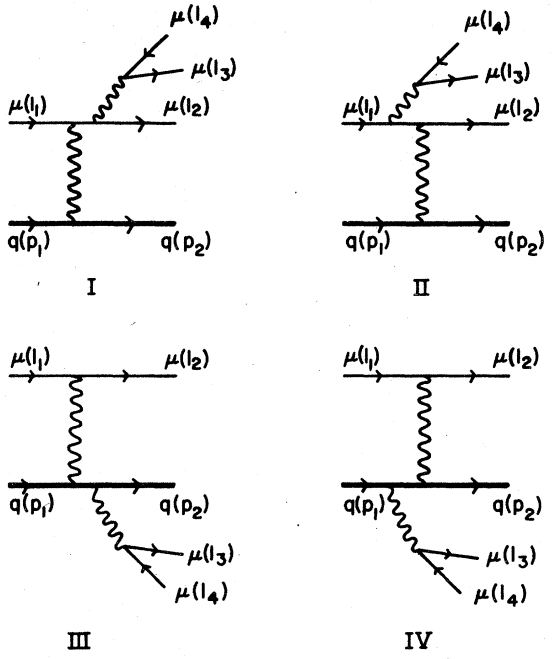

FIG. 5. Feynman diagrams for the reaction $\mu + q \rightarrow 3\mu + q$.

Since there seems to be no standard terminology,[15] we call the process depicted in Fig. 1(b) a muon radiative production, and the one in Fig. 1(c) a Compton production. The sum of these two processes we call the total production.

The diagrams investigated are shown in Fig. 5. We split the diagrams into two sets, each of which are separately gauge invariant. Namely, the cases when the pairs are produced from the muons and from the quarks. Denoting the matrix element of each of the four diagrams by M_{I}, M_{II}, M_{III}, and M_{IV} we have the following:

For muon radiative production, the amplitude

$$M_{\mathrm{I}} + M_{\mathrm{II}} = e^4 f \frac{1}{k^2} \frac{1}{p_y^{\,2}} \epsilon_\alpha \bar{u}(l_2) \left[\frac{(2l_{2\alpha} + \gamma_\alpha \not{k})}{k^2 + 2l_2 \cdot k} \gamma_\mu + \gamma_\mu \frac{(2l_{1\alpha} - \not{k}\gamma_\alpha)}{k^2 - 2l_1 \cdot k} \right] u(l_1) \bar{u}(p_2) \gamma_\mu u(p_1), \tag{1}$$

and for Compton production, the amplitude

$$M_{\mathrm{III}}+M_{\mathrm{IV}}=e^4f^2\,\frac{1}{k^2}\,\frac{1}{l_y^{\,2}}\,\epsilon_\alpha\,\bar{u}(l_2)\gamma_\mu u(l_1)\bar{u}(p_2)\left[\frac{(2p_{2\alpha}+\gamma_\alpha \not{k})}{k^2+2p_2\cdot k}\,\gamma_\mu+\gamma_\mu\,\frac{(2p_{1\alpha}-\not{k}\gamma_\alpha)}{k^2-2p_1\cdot k}\right]u(p_1) \tag{2}$$

where $k=l_3+l_4$, $p_y=p_1-p_2$, $l_y=l_1-l_2$, $\epsilon_\alpha=\bar{u}(l_3)\gamma_\alpha u(l_4)$, and the other momentum assignments are indicated in Fig. 5. f is the quark charge, when the u^- charge is taken as unity.

The program SCHOONSCHIP (Ref. 23) was used to evaluate the squares of the two matrix elements [Eqs. (1) and (2)] and the interference terms. By exploiting gauge invariance a reduction of the number of terms was possible. The matrix element was still rather large, and a regrouping of terms was carried out by hand, to reduce its size even further. The cross section for the reaction $\mu+q\to 3\mu+q$ takes the form

$$\sigma_q=\frac{1}{4}\,\frac{1}{2s}\,\frac{1}{(2\pi)^5}\,(4\pi\alpha)^4\int\frac{d^3l_2}{2E_2}\int\frac{d^3p_2}{2\omega_2}\int\frac{d^3k}{2E_k}\,\delta^4(l_1+p_1-l_2-k-p_2)\int dk^2\int\frac{d^3l_3}{2E_3}\,\frac{d^3l_4}{2E_4}\,\delta^4(k-l_3-l_4)\,|M^1|^2, \tag{3}$$

where the initial polarizations have been averaged and final polarizations summed over. M^1 is given by the relation $|M|^2=e^8|M^1|^2$. The integrations are carried out using methods described previously.[15]

So far we have not incorporated the effects of the quark-parton distributions. This is done by going to the center-of-mass frame, which at the energies considered is a fast moving frame. Here we scale the quark longitudinal momentum and neglect the muon mass. This leads to a scaling in the energy variable ($s\to xs$). Then we integrate the cross section given previously, over x, weighted by the structure function. This is just the naive parton model, and neglects any $p_\perp$ dependence of the quark structure function.

Since scattering occurs off both the u and d quarks we have for a proton

$$\sigma_p=\int[\sigma_u(x)u(x)+\sigma_d(x)d(x)]x\,dx\,, \tag{4}$$

and for a neutron

$$\sigma_n=\int[\sigma_u(x)d(x)+\sigma_d(x)u(x)]x\,dx\,, \tag{5}$$

where $\sigma_u(x)$, $\sigma_d(x)$ are the up- and down-quark cross sections at a given x.

We compute our cross section only for an isoscalar target for which we obtain

$$\sigma=\int(\sigma_u+\sigma_d)[d(x)+u(x)]\,x\,dx\,. \tag{6}$$

Our proton quark-parton distribution functions are[24]

$$F_2=x[u(x)+d(x)]_{\mathrm{val}}$$
$$=1.74\sqrt{x}\,(1-x)^3(1+2.3x)+1.11\sqrt{x}\,(1-x)^3\,, \tag{7}$$

and we neglected the sea contribution because it is very small. The matrix element is reasonably well behaved and the integrations were easily handled by the computer. Our calculations are accurate to approximately 10%.

III. DISTRIBUTIONS

In this section we discuss some of the distributions we obtained. As remarked previously, the diagrams where the muons radiate and where the quarks radiate are individually gauge invariant. This enables us to discuss the two processes separately, because the former is a pure quantum-electrodynamic background whereas the latter reveals information about the hadronic processes. Thus we present distributions for both processes, and point out the characteristic features of each. The emphasis is on being able to distinguish the two processes.

Qualitatively rather distinct differences exist between the two reactions. Since electrodynamic processes are maked by very low momentum transfers, the incident muon tends to come out at small angles (less than 1°) with a considerable fraction of its original energy. When the muon radiates it tends to do so with a hard photon,

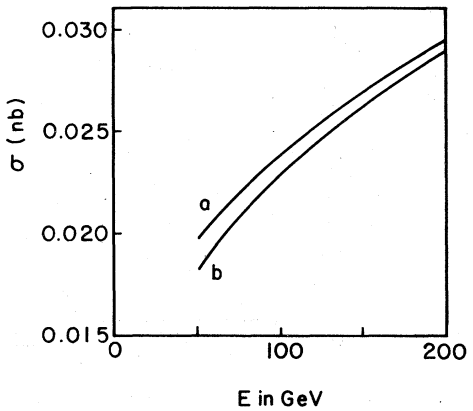

FIG. 6. Total cross section. Curve (a) is for total production, and curve (b) is for muon radiative production.

which, on becoming a muon pair, produces three muons with approximately equal energies. As the quarks do not have large energies imparted to them, when they radiate, the resulting muons have very low energies. Thus the former reaction tends to be characterized by three muons of comparable energy, while the latter reaction tends to have a very fast muon ($\langle p\rangle = 185$ GeV at 200 GeV) and a pair of very slow muons ($\langle p\rangle = 4$ GeV at 200 GeV). This enables us to understand many features of the distributions.

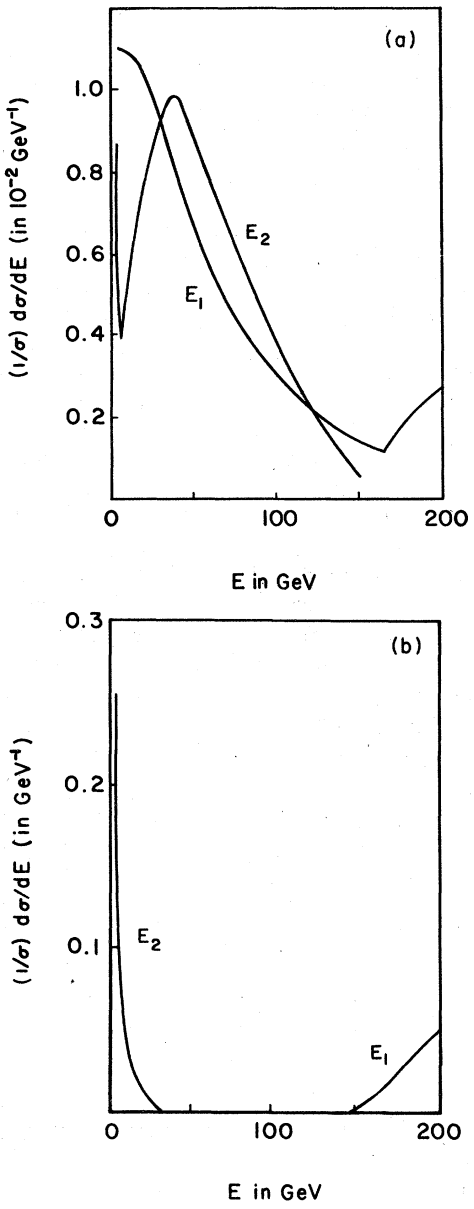

FIG. 7. Energy spectrum of muons at $E = 200$ GeV: (a) total production, (b) Compton production.

We now present in detail the various differential cross sections. We have not incorporated any cuts, and have not used any criterion to distinguish between the two identical muons. The criterion used in neutrino collisions does not seem very appropriate here, because the hadron energies are low, and hence the hadron direction does not convey much information. When experimental cuts and criteria for selection are used we can easily incorporate them in our computer program.

We computed the cross sections for negatively charged muons, at muon laboratory energies of 50, 100, and 200 GeV. We present the differential cross sections at 200 GeV in detail and indicate where necessary, any differences at other energies. In the diagrams calculated, we find that about 95% of the total cross section arises from the muon radiation. For example, at 200 GeV we have 2.95×10^{-35} cm^2 for the muon-radiative-production cross section and 1.5×10^{-36} cm^2 for the Compton-production cross section. Thus most of the features manifested by the total production cross section are characteristic of muon radiation only. Hence only the total and Compton production distributions will be presented. Differences will be indicated where appropriate.

The cross sections for the total production and the muon radiative production are shown in Fig. 6. The Compton production was found to be about 5% of the total production in the energy range shown. All cross sections have a rather slow rise with energy, as contrasted with the neutrino case where the electromagnetic trimuon production cross section increases as $E\ln^2 E$.[15] We denote the prompt negatively charged muon by 1 ("fast"),

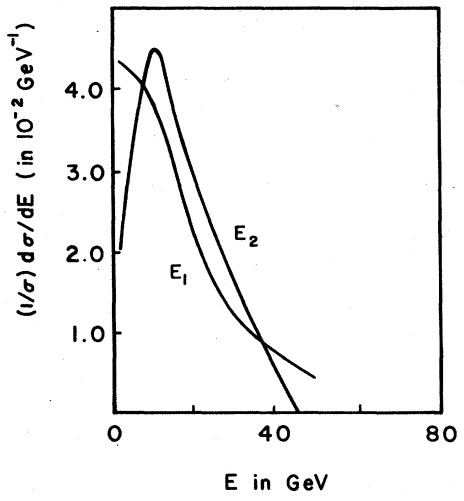

FIG. 8. Energy spectrum of muons at $E = 50$ GeV. Total production.

the negative muon which is pair produced by 2 ("slow"), and the positive muon by 3. Since we have used no criterion for distinguishing the muons, the distributions are identical for muons 2 and 3.

We present the energy spectrum for the three muons in Fig. 7 for $E = 200$ GeV. The interesting feature is that the Compton diagrams provide a rise above the muon radiation diagrams at the high- and low-energy end of the spectrum. [Fig. 7(a)]. This feature disappears at lower muon laboratory energies as is seen in Fig. 8, which is for $E = 50$ GeV.

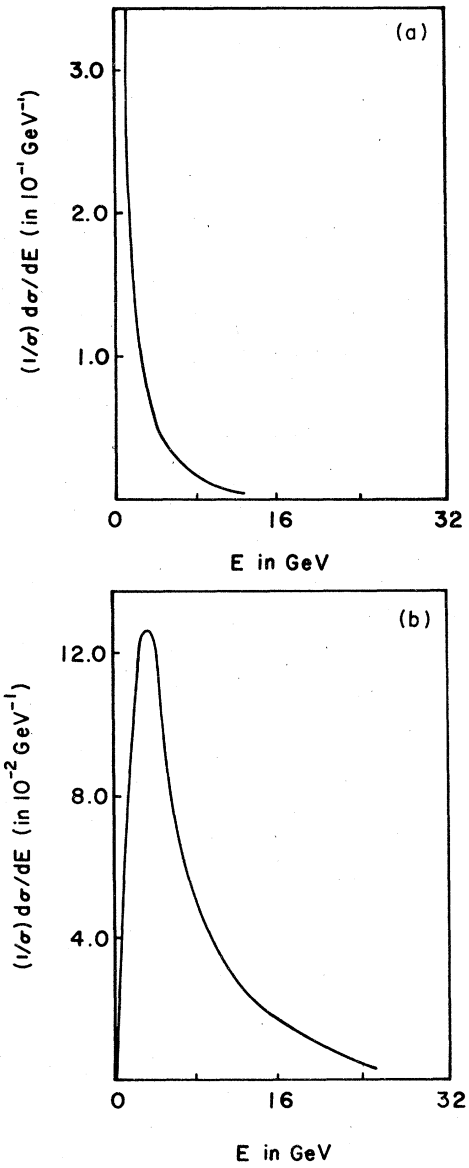

FIG. 9. Energy spectrum of hadrons at $E = 200$ GeV. (a) total production, (b) Compton production.

The hadron energy distributions are shown in Fig. 9. As expected for quantum-electrodynamic processes, the energy transferred to the hadrons is very low. The average hadronic energy for the total process is 2.2 GeV, which is much lower than that for the Compton process, 5.8 GeV. This is easily understood, because the faster-moving hadrons are more likely to radiate muon pairs.

We show the various invariant-mass distributions of the muons in Fig. 10. In both cases the

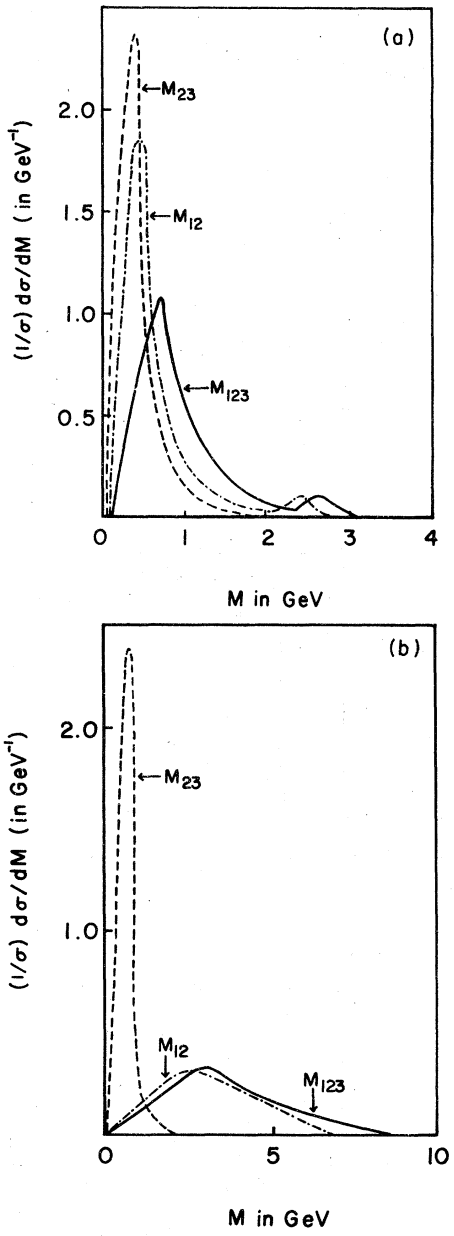

FIG. 10. Invariant-mass distributions for the muons at $E = 200$ GeV. (a) total production, (b) Compton production.

invariant mass of particles 2 and 3 (M_{23}) is peaked at very low values, arising from the infrared divergent nature of electrodynamic processes. Marked differences arise in the invariant-mass distributions of the "fast" muon with either of the "slow" muons (M_{12} or M_{13}), and in the invariant mass of the three muons (M_{123}). The case when the radiation occurs off the muons tends to have lower invariant mass (below 2 GeV) as compared to quark radiation (up to about 6 GeV). This effect can be seen in the bump arising at about 2.5 GeV, in M_{12} and M_{123} [Fig. 10(a)]. This may provide a possible cut to study the Compton process.

Shown in Fig. 11 are the invariant-mass distributions of the hadrons and the two muons which are pair-produced (W of a single-particle inclusive reaction). In muon radiative production, the two muons move away from the hadrons, with a large momentum. Thus the invariant masses are higher, as compared with Compton production, where the hadrons and muons tend to move together, giving lower invariant masses.

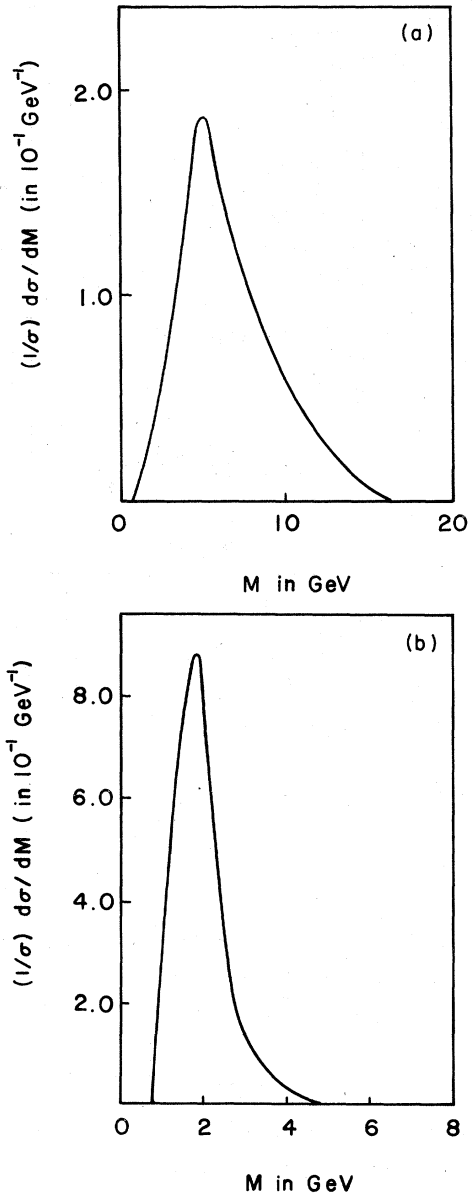

FIG. 11. Invariant-mass distribution of hadrons and slow muons at $E = 200$ GeV. (a) total production, (b) Compton production.

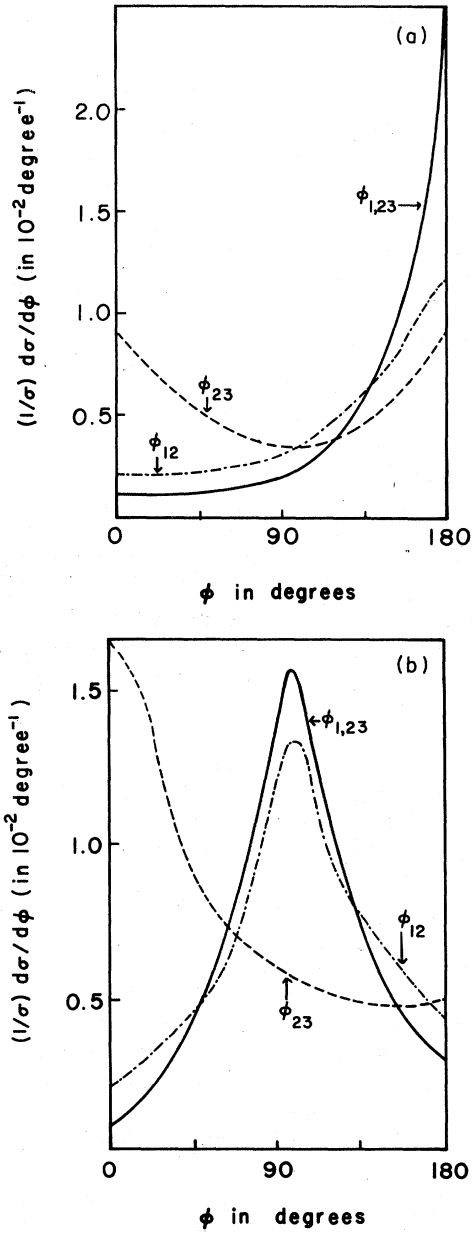

FIG. 12. Distributions in the ϕ angles at $E = 200$ GeV. (a) total production, (b) Compton production.

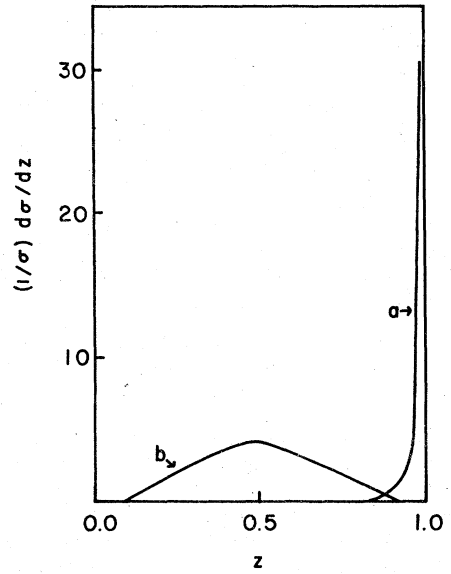

FIG. 13. Distribution in the z variable at $E = 200$ GeV. Curve (a) is for total production, and curve (b) is for Compton production.

We consider next the distributions in the opening angles of the final muon momentum vectors projected on a plane perpendicular to the incident muon direction (Fig. 12). These are the ϕ angles between various particles, and they have proven to be important in understanding trimuon production by neutrinos. For the total and also the muon pair production [Fig. 12(a)] we note a peaking of $\phi_{12}(\equiv\phi_{13})$ in the backward direction. For $\phi_{1,23}$ we see an even more severe peaking in the backward direction. This is a key characteristic of muon radiative production. Unlike the case of neutrino scattering, the hadron shower does not carry a lot of momentum, hence the muon is deflected only a little, carrying a large parallel momentum. Thus when it radiates, the pair tends to move in the opposite directions to conserve transverse momentum. For the Compton production we see that ϕ_{12}, ϕ_{13}, and $\phi_{1,23}$ are peaked around 90°. ϕ_{23} is peaked at low angles.

The transverse momenta of the muons are small. The averages are about 0.3 GeV for all the muons, over the energy range considered. Correlated with this are the opening angles between the muons. For muon radiative production the opening angles are all less than 0.25°. For Compton production we obtain 71% of the cross section below 0.25°, 90% below 0.5°, and 98% below 0.75°. The average opening angles are 0.35°.

Another quantity of interest is the z variable which is defined as $z = (E_2 + E_3)/(E_{\text{had}} + E_2 + E_3)$, and distributions in this variable are shown in Fig. 13. For muon radiative production the distribution peaks at values of z close to 1. This is so because the hadron energy is low relative to the muon energies. In contrast for Compton production the hadrons and muons share the energy, and hence the distribution peaks in the middle.

We have presented distributions in some variables which contrast the behavior of muon radiative and Compton production processes. As noted, these distributions were obtained without using any experimental cuts. These will change some distributions rather dramatically. Thus some of the features shown may not be manifest in raw experimental data.

IV. CONCLUSIONS

As mentioned, we have attempted to contrast the Compton production with the muon radiative production to see if the former can be observed and studied. Now, one of the most obvious and for this reaction a very severe cut is the one in energy. Muons of energy lower than about 4 GeV are not observed, as detectors require that energy to register. Turning to the energy distributions for the Compton process [Fig. 7(b)], we see that the two pair produced muons have an average energy of only 4 GeV. Thus a large portion of events will not be observed as trimuon events. This could be a reason why in previous experiments there was no need for this process to explain the events.

Thus the problem arises of trying to observe these events. Many of them appear as single-muon events. However, when the experimental situation is clarified further, it may be possible to give additional criteria to distinguish these events.

The other distribution shown can also be used to identify these events. Though the energy cuts lower the rates, the z distributions may still be helpful in identifying the events.

We conclude by saying that we need to await data before beginning to unravel trimuon production. We have discussed one possible source of events which we expect to be present.

ACKNOWLEDGMENT

This work is supported in part by the National Science Foundation under Grant No. PHY-76-15328.

[1]This work has been reviewed by E. G. Johnson Jr., Phys. Rev. 140, B1005 (1965).
[2]S. J. Brodsky and S. C. C. Ting, Phys. Rev. 145, 1018 (1966).
[3]M. J. Tannenbaum, Phys. Rev. 167, 1308 (1967).
[4]J. J. Russell *et al.*, Phys. Rev. Lett. 26, 46 (1971).
[5]R. P. Feynman, *Photon-Hadron Interactions* (Banjamin, New York, 1972); J. D. Bjorken and E. A. Paschos, Phys. Rev. 185, 1975 (1969).
[6]J. D. Bjorken and E. A. Paschos, Phys. Rev. D 1, 1450 (1970).
[7]J. F. Davis *et al.*, Phys. Rev. Lett. 19, 1356 (1972).
[8]D. O. Caldwell *et al.*, Phys. Rev. Lett. 33, 868 (1974).
[9]H. Deden *et al.*, Nucl. Phys. B85, 269 (1975).
[10]See, for example, B. C. Barish, Phys. Rep. 39C, 279 (1978).
[11]B. C. Barish *et al.*, Phys. Rev. Lett. 38, 557 (1977).
[12]A. Benvenuti *et al.*, Phys. Rev. Lett. 38, 1110 (1977); A. Benvenuti *et al.*, *ibid.* 40, 488 (1977).
[13]M. Holder *et al.*, Phys. Lett. 70B, 393 (1977).
[14]See, for example, J. Smith, Invited Talk at the International Neutrino Physics Conference (Purdue, 1978) [Stony Brook Report No. ITP-SB-78-31 (unpublished)].
[15]J. Smith and J. A. M. Vermaseren, Phys. Rev. D 17, 2288 (1978).
[16]V. Borger, T. Gottschalk, and R. J. N. Phillips, Phys. Rev. D 17, 2284 (1978); R. M. Barnett, L. N. Chang and N. Weiss, *ibid.* 17, 2266 (1978).
[17]T. Hansl *et al.*, CERN reports, 1978 (unpublished).
[18]C. Chang, K. W. Chen, and A. van Ginneken, Phys. Rev. Lett. 39, 519 (1977); *Proceedings of the International Symposium on Lepton and Photon Interactions at High Energies, Hamburg, 1977,* edited by F. Gutbrod (DESY, Hamburg, 1977), p. 467.
[19]F. Bletzacker, H. T. Nieh, and A. Soni, Phys. Rev. Lett. 38, 1241 (1977); F. Bletzacker and H. T. Nieh, Stony Brook Report No. ITP-SB-77-42 (unpublished).
[20]L. M. Jones and H. W. Wyld, Phys. Rev. D 17, 759 (1978).
[21]See also G. Kane, J. Smith, and J. A. M. Vermaseren, Phys. Rev. D (to be published), for further references.
[22]G. G. Henry, Ph.D. thesis, University of Chicago, 1978 (unpublished).
[23]SCHOONSCHIP is an algebraic program written by M. Veltman. See H. Strubbe, Comput. Phys. Commun. 8, 1 (1974).
[24]J. Okada, S. Pakvasa, and S. F. Tuan, Lett. Nuovo Cimento 16, 555 (1976); See also R. D. Field and R. P. Feynman, Phys. Rev. D 15, 2590 (1977) for an alternate parametrization.